Journal of Analytical and Applied Pyrolysis 120 (2016) 52–59

Contents lists available at ScienceDirect

Journal of Analytical and Applied Pyrolysis

journal homepage: www.elsevier.com/locate/jaap

Effects of oxygen-containing substituents on pyrolysis characteristics of β-O-4 type model compounds

Pan Li[a], Lei Chen[b], Xianhua Wang[a,*], Haiping Yang[a], Jingai Shao[a], Hanping Chen[a]

[a] State Key Laboratory of Coal Combustion, Huazhong University of Science & Technology, Wuhan 430074, Hubei, PR China
[b] Key Laboratory of Thermo-Fluid Science and Engineering of Education Ministry, Xi'an Jiaotong University, Xi'an, Shanxi,710049, PR China

ARTICLE INFO

Article history:
Received 11 December 2015
Received in revised form 18 April 2016
Accepted 21 April 2016
Available online 27 April 2016

Keywords:
β-O-4 model compounds
Pyrolysis characteristics
Temperature
Py-GC–MS

ABSTRACT

In order to uncover the influence of oxygen-containing functional groups on the pyrolysis characteristics of β-O-4 type model compounds, in-situ diffuse reflectance infrared pyrolysis and pyroprobe-GC–MS were used to study the migration patterns of functional groups and the specific pyrolysis product distributions with changing temperature. The results showed that the initial temperature of phenolic hydroxy production was 300 °C, and peaks corresponding to this increased gradually in intensity in 1-benzyl-2-(2-methoxy-phenol)-ethanol, while this product did not begin appearing until 600 °C in 1-ethyl-benzene-2-(2-methoxy-phenol). The intensities of the CH_4 peaks were similar in all three samples, but the CO_2 absorption peak was significantly lower in 1-(4-methoxy-phenoxy)-2-(2-methoxy-phenol)-ethanol. In addition, α-OH was found to promote the generation of aryl-ketone products. The 4-methoxy-styrene contents of 1-ethyl-benzene-2-(2-methoxy-phenol) and 1-(4-methoxy-phenoxy)-2-(2-methoxy-phenol)-ethanol at 500 °C were 36.1% and 31.3%, respectively, higher than the styrene content of 1-benzyl-2-(2-methoxy-phenol)-ethanol (26.3%). The content of acetophenone was only 0.3% in 1-ethyl-benzene-2-(2-methoxy-phenol), but the yields of acetophenone and 4-methoxy-acetophenone were 16.7% and 19.6% in 1-benzyl-2-(2-methoxy-phenol)-ethanol and 1-(4-methoxy-phenoxy)-2-(2-methoxy-phenol)-ethanol, respectively.

1. Introduction

In response to energy needs, urban development and environmental pollution, and other social problems, the exploitation and utilization of biomass energy has been of extensive concern, with research and development of biomass conversion technology becoming a focus of worldwide efforts [1,2]. As an important means of thermochemical conversion, pyrolysis can be used to convert biomass to high-grade fuels and chemical products, as well as to provide theoretical support for combustion, gasification, and liquefaction technologies [3,4].

The main components of biomass are cellulose, hemicellulose, lignin, and trace amounts of extracts [5]. After cellulose, lignin is the second most abundant organic polymer in terrestrial plants, and it is composed of three basic structural units: *p*-hydroxyphenyl propane, guaiacyl propane, and syringyl propane [6]. Because of its unique chemical structure, lignin is a feasible raw material for the production of valuable chemicals and medicines by tailoring the molecules produced by its pyrolysis. The bonds between the monomers are predominantly ether linkages (α- and β-ether bonds) and condensed carbon—carbon bonds (aryl-aryl, β-aryl, and β-β) [7,8]. β-O-4 bonds account for 48–60% of total lignin linkages [9]; therefore, mastering the pyrolysis mechanism of β-O-4 type model compounds will contribute to a complete understanding of lignin pyrolysis. For this reason, research on pyrolysis of β-O-4 type model compounds has attracted the interest of a large number of researchers. Chu et al. [10] studied the pyrolysis behavior of a β-O-4 type oligomeric lignin model compound between 250 °C and 550 °C, and found that the β-O-4 linkage thermally decomposed between 250 °C and 350 °C with the formation of solid products at 350 °C. The most abundant monomeric product was 2-methoxy-4-methyl phenol, with char also being formed, most likely by random re-polymerization of the radicals as temperature increased. Britt et al. [11] studied the rapid vacuum pyrolysis of phenethyl phenyl ether (PPE) and proposed a complex reaction pathway which was dominated by free-radical reactions, molecular rearrangements, and concerted elimination reactions and explained the high yields of styrene and phenol products. Huang et al. [12] studied the mechanism of pyrolysis of β-O-4 model compounds using density functional theory and showed that there were three pyrolysis path-

* Corresponding author.
E-mail address: wxhwhhy@sina.com (X. Wang).

http://dx.doi.org/10.1016/j.jaap.2016.04.009
0165-2370/

ways, and that at low temperature pyrolysis was mainly dominated by concerted reactions while at high temperature free-radical reactions (Cβ-O homolytic reactions) were dominant. However, with different side chains or substituted groups, the mechanism of pyrolysis may change. Kawamoto et al. [13] have studied the influence of C_γ–OH on the pyrolytic cleavage mechanism of β-ether linkages in lignin dimers and proposed that introducing OH at the C_γ position changed the β-ether cleavage mechanism in the phenolic form from a radical chain mechanism to a quinone methide mechanism. Hydroxy and methoxy groups are common substituents in lignin structures [14], and so clearly more research is needed to understand their roles. Studying the pyrolysis characteristics of β-O-4 type model compounds with different substituents is therefore of great significance for the in-depth understanding of lignin pyrolysis. However, little research has been done on the effects of oxygen-containing substituents on the pyrolysis characteristics of β-O-4 type model compounds, with work mostly focusing on theoretical decomposition routes.

Herein, the effects of α-OH and *p*-methoxy groups on the pyrolysis characteristics of β-O-4 model compounds were investigated by using an in-situ diffuse reflectance infrared pyrolysis system to explore the migration patterns of volatile functional groups with temperature changes, and a pyroprobe-GC–MS system to investigate the specific pyrolysis product distributions yielded by different oxygen-containing substituents. This provided useful information for the understanding of the impact of substituent groups on the pyrolysis pathway.

2. Experimental

2.1. Samples

In this study, the β-O-4 type model compounds with oxygen-containing substituents used were:

(1) 1-Ethyl-benzene-2-(2-methoxy-phenol), referred to as (*p*-methoxy-PPE-(*o*-OMe));
(2) 1-Benzyl-2-(2-methoxy-phenol)-ethanol, referred to as (α-OH-PPE-(*o*-OMe));
(3) 1-(4-Methoxy-phenoxy)-2-(2-methoxy-phenol)-ethanol, referred to as ((*p*-methoxy + α-OH)-PPE-(*o*-OMe)).

The molecular structures of these compounds are shown in Fig. 1, and the specific synthetic route and characterization data can be found in related literature [15,16].

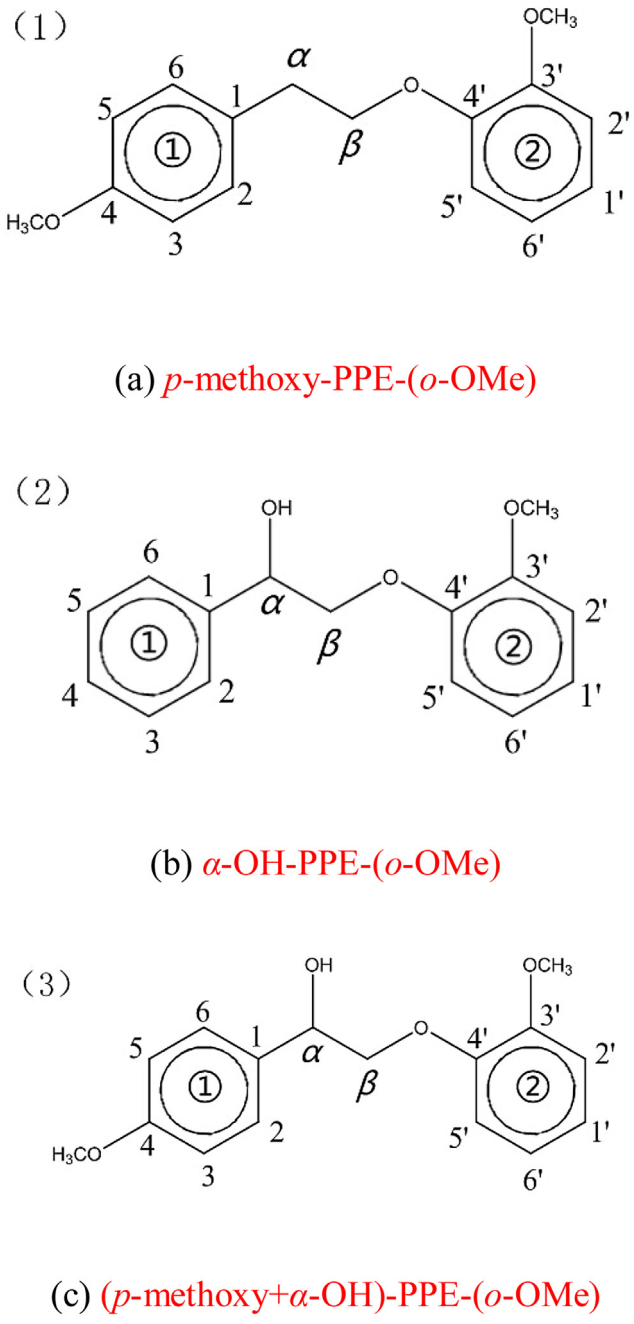

Fig. 1. Molecular structures of the three model compounds.

2.2. Experimental method

2.2.1. In-situ diffuse reflectance infrared pyrolysis system

The in-situ diffuse reflectance infrared pyrolysis system used Fourier transform infrared spectroscopy (Nicolet IS50, Thermo Fisher Scientific Company, USA) and an in-situ pool with a deuterated sulfuric acid GSH detector. In order to ensure full beam transmittance and good heat resistance, CaF_2 with protective water-cooling was used for the window. The real-time temperature of the in-situ pool was adjusted using a temperature controller with a PID (proportion, integration and differentiation) thermocoupling controller, and the accuracy of the temperature control was ±1 °C. Specific operation parameters were as follows: nitrogen with purity of 99.999% was used to purge the system at a rate of 1 L/min for 15 min to maintain an inert atmosphere, after which the intake and outlet valves were closed to ensure that the pyrolysis process was carried out under sealed conditions. The temperature was increased from room temperature to 670 °C at a rate of 40 °C/min and was held at 670 °C for 10 min. The spectral scanning range was 400–4000 cm^{-1}, the resolution was 4 cm^{-1}, and the sampling interval was 1.93 s. A N_2 atmosphere at 100 °C was selected as the spectral background.

2.2.2. Pyroprobe-GC–MS

Rapid pyrolysis of the three materials in was performed in a pyrolyzer (CDS 5200HP, CDS company, USA), and the obtained volatiles were analyzed using GC–MS (Clarus 560, PE company, USA). Specific operation parameters were as follows: 10 mg of samples were placed in 100 mL anhydrous ethanol and well mixed. During each test, 10 μL of sample solution, as measured using a locking syringe, was injected into the quartz wool of the reactor tube to give a sample weight of 1 μg. Before the experiment, the system was purged using the carrier gas (helium, 99.999%) for 1 min to remove the anhydrous ethanol. The selected temperatures

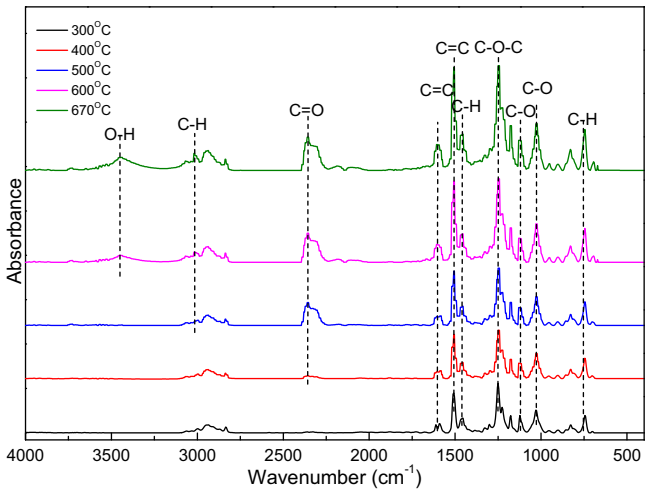

Fig. 2. The temperature-dependent infrared spectral distributions of *p*-methoxy-PPE-(*o*-OMe).

Table 1
Organic functional groups detected by FT-IR.

Wave number/cm^{-1}	Absorption peak	Functional group & structure
3460–3412	O—H Stretching vibration	Phenolic hydroxyl
3000–2842	C—H Stretching vibration	Methyl and methylene
2350–2358	C=O Stretching vibration	Carbon dioxide
1660–1720	C=O Stretching vibration	Aromatic ketone
1500–1620	C=C Stretching vibration	Aromatic
1420–1480	C—H Bending vibration	Methoxy
1200–1300	C—O—C Stretching vibration	Aromatic ether
1000–1150	C—O Stretching vibration	Hydroxy
625–1000	C—H Bending vibration	Olefin and aromatic

were 500 °C and 800 °C, the pyrolysis time was 20 s, and the heating rate was 20 °C/ms. The main components of the bio-oil were identified using a GC–MS equipped with a capillary column (Elite-35MS; length, 30 m; internal diameter, 250 μm; film thickness, 0.25 μm). The temperature of the injection valve and the transmission pipeline for the pyrolysis products were set to 300 °C. The GC oven temperature was initially set to 40 °C, then heated to 280 °C at a rate of 15 °C/min, and it was held at this temperature for 2 min. The injector temperature was 280 °C, and the split ratio was 80:1. The software GG1034C Chemstation (with a National Bureau of Standards Library) was used to identify each compound based on the retention time and by matching the mass spectrum with the standards in the spectral library.

3. Results and discussion

3.1. Analysis of in-operando FT-IR experiments

Analysis of the variations of the volatile small molecules produced during the pyrolysis of the model compounds, with changing temperature was performed using the in-situ diffuse reflectance infrared pyrolysis device. This enabled real-time monitoring, with *p*-methoxy-PPE-(*o*-OMe)'s results being displayed in Fig. 2.

The main functional groups of three samples are listed in Table 1. As shown in Fig. 2, the peak at around 3452 cm^{-1} was due to the

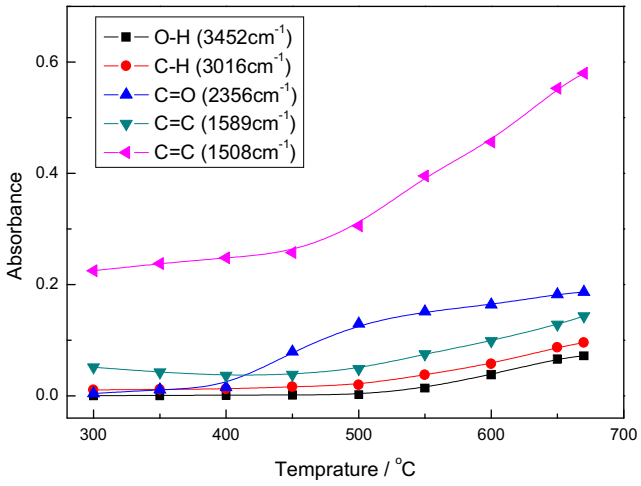

(a) IR peak intensities in the region 4000 cm^{-1}–1500 cm^{-1}

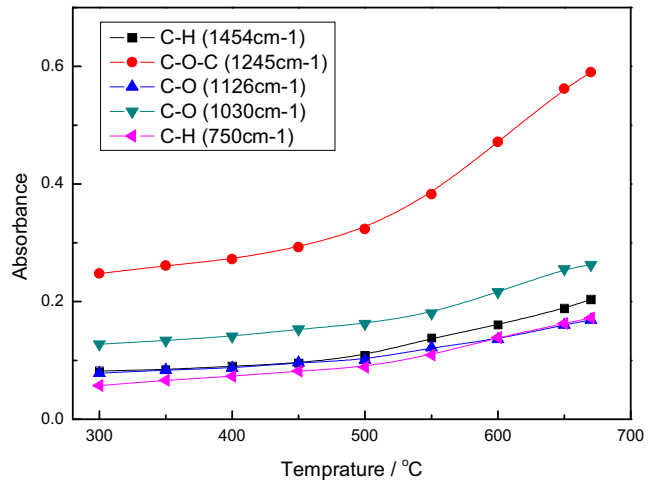

(b) IR peak intensities in the region 1500 cm^{-1}–500 cm^{-1}

Fig. 3. Variation in absorption intensity with temperature for *p*-methoxy-PPE-(*o*-OMe).

phenolic hydroxyl group, that at 3016 cm^{-1} represents the methyl and methylene groups, which will be referred to as CH_4 from hereon. Next, the peak at around 2356 cm^{-1} indicates CO_2 absorption, while those at 1677 cm^{-1} and 1681 cm^{-1} show the presence of aromatic ketone substances. After this, there follows benzene derivatives with a single substituent (around 1590 cm^{-1}), peaks corresponding to the aromatic framework (around 1508 cm^{-1}), O—CH_3 (around 1455 cm^{-1}), and aromatic ethers (1245 cm^{-1}) Peaks indicating carbon-hydroxyl bonds can be seen at around 1125 cm^{-1} and 1030 cm^{-1}, and those showing olefin/aromatic substances at around 750 cm^{-1}.

According to Lambert-Beer's law, the absorbance level at a particular wave number represents the concentration of a substance; therefore, changes in absorbance intensity can reflect the varying concentrations of volatile gases during pyrolysis. Thus, the

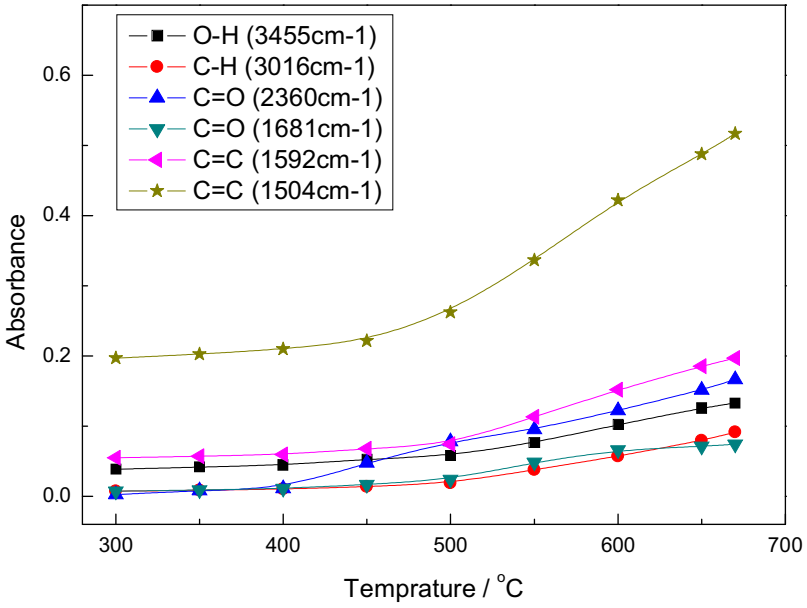

(a) IR peak intensities in the region 4000 cm^{-1}–1500 cm^{-1}

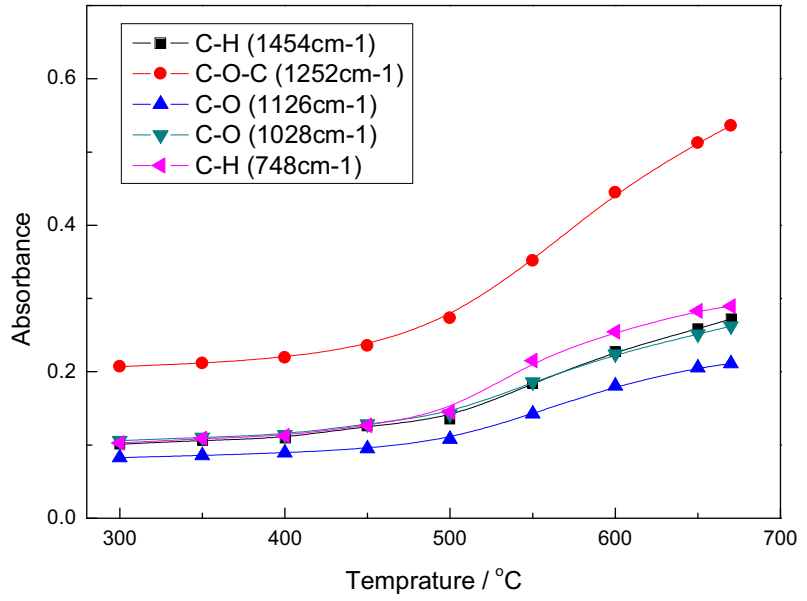

(b) IR peak intensities in the region 1500 cm^{-1}–500 cm^{-1}

Fig. 4. Variation in absorption intensity with temperature for α-OH-PPE-(*o*-OMe).

changes in absorbance corresponding to specific functional groups at different temperatures were analyzed semi-quantitatively using the height of the IR peaks for the three samples, as shown in Figs. 3–5 .

For *p*-methoxy-PPE-(*o*-OMe) (shown in Fig. 3(a)), the intramolecular hydrogen bond vibration of the phenolic hydroxy functional groups was detected from 550 °C, with the peak intensity increasing with temperature. The peak corresponding to the

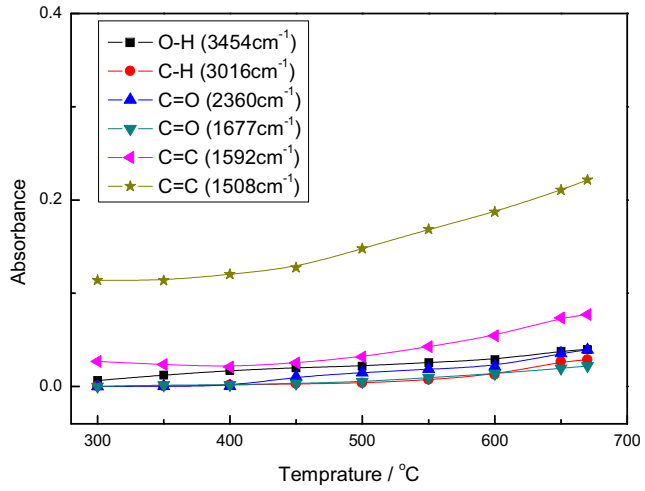

(a) IR peak intensities in the region 4000 cm^{-1}–1500 cm^{-1}

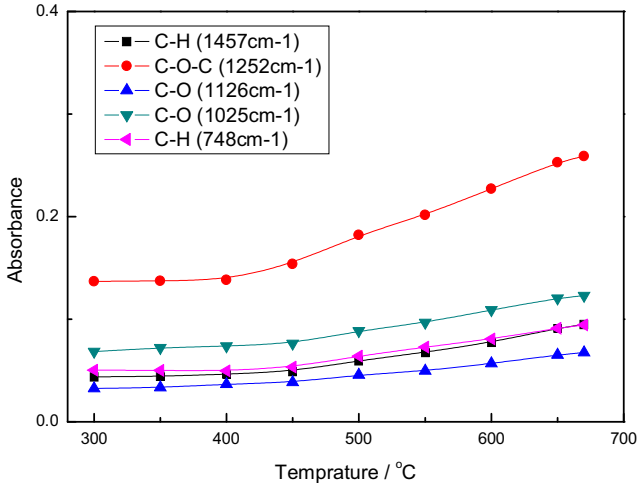

(b) IR peak intensities in the region 1500 cm^{-1}–500 cm^{-1}

Fig. 5. Variation in absorption intensity with temperature for (*p*-methoxy + α-OH)-PPE-(*o*-OMe).

emission of CH_4 [17,18], which appeared at about 500 °C, also gradually increased in intensity with rising temperature. The intensity of the CO_2 absorption peak grew rapidly between 400 °C and 500 °C, and then began to level off at higher temperatures, which indicated that CO_2 was generated before 500 °C during the pyrolysis progress and that its yield was higher than that of CH_4. The peak caused by C=C stretching vibrations in mono-substituted benzenes and aromatic frameworks showed no significant changes between 300 and 450 °C, but it rapidly increased between 450 and 670 °C. From Fig. 3(b), the concentrations of O—CH_3 and O—H groups, aromatic ethers, and hydrocarbons all gradually increased with temperature, particularly above 500 °C. In addition, the aromatic ether peak (1245 cm^{-1}) was much stronger than the others were.

The variation in intensity of α-OH-PPE-(*o*-OMe) peaks with temperature is shown in Fig. 4. From Fig. 4(a), it can be seen that the phenolic hydroxy group existed throughout the temperature range 300–670 °C, which was different to what was seen for *p*-methoxy-PPE-(*o*-OMe). The yield of CH_4 gradually increased with temperature above 500 °C, but the overall concentration was relatively small. The intensity of CO_2 increased continuously from 400 °C to 670 °C, but the yield was lower than for *p*-methoxy-PPE-(*o*-OMe). The peak corresponding to aromatic ketones became stronger at higher temperatures, which showed that the generation of aryl-ketone products occurred after 500 °C and their yield gradually increased. While other peaks mentioned in Table 1 were also enhanced when pyrolysis temperature was increased, especially between 500 and 670 °C, the intensity of the peak corresponding to the C—O—C structure was still the largest, as shown in Fig. 4(b).

In Fig. 5(a), it can be seen that only the peaks corresponding to the aromatic framework (1592 cm^{-1} and 1508 cm^{-1}) increased significantly above 500 °C, with other substances such as aromatic ketones, benzene derivatives, CH_4, and CO_2 only showing a slight increase. In Fig. 5(b), it can be seen that the amount of all the substances listed in Table 1 increased throughout the heating process, with aromatic ether substances standing out overall. However, the overall intensity of the functional groups in (*p*-methoxy + α-OH)-PPE-(*o*-OMe) was relatively low.

During α-OH-PPE-(*o*-OMe) pyrolysis the –OH peak initially appeared at a temperature of 300 °C, after which its intensity gradually increased, while in *p*-methoxy-PPE-(*o*-OMe) its appeared at 600 °C with only a weak, small peak being obtained at 670 °C. The CH_4 emission peak was similar in three samples, beginning at about 500 °C and intensifying with increasing temperature. This indicates that the demethylation reaction began at 500 °C. However, the intensity of the CO_2 absorption peak in α-OH-PPE-(*o*-OMe) and *p*-methoxy-PPE-(*o*-OMe) was significantly higher than in (*p*-methoxy + α-OH)-PPE-(*o*-OMe). This could be attributed to the steric hindrance due to the co-existence of the α-OH and *p*-methoxy groups, which may have inhibited the decarbonylation. In contrast with the other materials, no aryl-ketone peak appeared during the pyrolysis of *p*-methoxy-PPE-(*o*-OMe), which showed that the introduction of α-OH groups could promote the generation of aryl-ketone products. The peaks around 1582 cm^{-1} were significantly enhanced above 500 °C in all three samples, indicating that more mono-substituted benzenes were being obtained. The O—CH_3 peak remained stable between 300 and 500 °C then rapidly increased in intensity, indicating that methoxy restructuring and homolytic reactions occurred after 500 °C [19,20], while the trends in O—H peak intensity were similar in all the samples. However, as temperature increased, especially to above 500 °C, more olefin and aromatic products were obtained from pyrolysis of α-OH-PPE-(*o*-OMe) than for the other two materials.

3.2. Results of rapid pyrolysis with pyroprobe-GC–MS

The pyrolysis results of the three samples at 500 °C and 800 °C, as calculated according to the detected organic products and their relative peak areas, are shown in Table 2. For the pyrolysis of *p*-methoxy-PPE-(*o*-OMe), the main products were 2-hydroxybenzaldehyde (14.4%), phenol (5%), 2-cresol (7.5%), guaiacol (6.7%), 4-ethyl-anisole (13.0%). and 4-methoxy-styrene (36.1%) at 500 °C, with no detectable generation of benzene. When the temperature was increased to 800 °C, the benzene yield rose to 28.4%, and the content of 4-methoxy-styrene decreased to 13.6%. At the same time, the 4-ethyl-anisole content decreased from 13% at 500 °C to 2.4% at 800 °C, indicating that aromatic hydrocarbons with oxygen-containing functional groups as chains are unstable at high temperature, with secondary cracking reactions occurring to generate aromatics products with single, relatively simple sub-

Table 2
Pyrolysis product distribution at various temperatures.

No.	Compounds	Formula	*p*-Methoxy-PPE-(*o*-OMe)		α-OH-PPE-(*o*-OMe)		(*p*-Methoxy + α-OH)-PPE-(*o*-OMe)	
			500 °C	800 °C	500 °C	800 °C	500 °C	800 °C
1	Benzene	C_6H_6	–	28.4	–	5.5	–	–
2	Toluene	C_7H_8	1.3	4.2	–	2.8	–	3.2
3	Ethylbenzene	C_8H_{10}	0.4	1.6	1.6	2.5	–	0.7
4	Styrene	C_8H_8	1.1	3.4	26.3	27	–	2.7
5	Anisole	C_7H_8O	3.1	2	–	0.3	–	2.2
6	Benzaldehyde	C_7H_6O	0.8	1.2	6.7	5.9	–	2.0
7	Phenol	C_6H_6O	5	10	4	9.3	–	17.1
8	Phenylacetate	C_8H_8O	–	–	5.5	2.7	–	–
9	2-Hydroxy-benzaldehyde	$C_7H_6O_2$	14.4	13.9	11.7	16.1	20.2	15.3
10	2-Cresol	C_7H_8O	7.5	2.1	3.8	3.2	–	5.1
11	Acetophenone	C_8H_8O	0.3	4.3	16.7	16.5	–	1.4
12	3-Methyl-phenol	C_7H_8O	–	–	–	–	–	2.1
13	Guaiacol	$C_7H_8O_2$	6.7	2.2	10.4	4.3	8.1	1.7
14	4-Ethyl-anisole	$C_9H_{12}O$	13.0	2.4	–	–	–	–
15	2-Ethyl-phenol	$C_8H_{10}O$	2.4	1.4	0.8	0.1	–	1.4
16	4-Methoxy-styrene	$C_9H_{10}O$	36.1	13.6	0.7	1.4	31.3	9.9
17	*P*-Ethyl-phenol	$C_8H_{10}O$	3.1	2.8	–	–	–	2.5
18	Benzoic acid	$C_7H_6O_2$	–	–	9	0.6	–	–
19	4-Ethyl-benzaldehyde	$C_9H_{10}O$	0.9	2.9	–	–	–	–
20	4-Vinyl-phenol	C_8H_8O	–	–	–	–	–	12.1
21	2-Methoxy benzaldehyde	$C_8H_8O_2$	–	–	2.8	1.7	–	1.3
22	4-*n*-Propylphenol	$C_8H_8O_2$	3.9	3.5	–	–	–	–
23	4-Methoxy-benzaldehyde	$C_8H_8O_2$	–	–	–	–	4.1	3.2
24	4-Methoxy-acetophenone	$C_9H_{10}O_2$	–	–	–	–	19.6	11.4
25	4-Hydroxy-acetophenone	$C_8H_8O_2$	–	–	–	–	15.7	4.6

stituents [21]. This led to increased yields of benzene, toluene, ethylbenzene, styrene, etc., at higher temperatures. There were also higher yields of phenol (10%), but lower yields of 2-cresol (2.2%) and guaiacol (2.1%), which could be due to phenolic compounds with multiple substituents being converted to phenol at 800 °C [22]. For pyrolysis of α-OH-PPE-(*o*-OMe) at 500 °C, the main products were styrene (26.3%), benzaldehyde (6.7%), 2-hydroxy-benzaldehyde (11.7%), acetophenone (16.7%), guaiacol (10.4%), and benzoic acid (9%), which was consistent with the results of in-situ FT-IR. The styrene content was 27% at 800 °C, which was almost the same as obtained at the lower temperature. The main route for styrene production was through Cβ-O homolytic reactions of the model compound, first via ether bond cleavage, then a dehydroxylation reaction [23], and these can likely be carried out at 500 °C. Guaiacol was also an important product, mainly being formed through combination of the model compounds with free H radicals after Cβ-O homolytic reaction [20,24], whereas, when the temperature was raised to 800 °C, the yield of guaiacol was greatly reduced, to 4.3%. The content of 2-hydroxy-benzaldehyde was 11.7% at 500 °C, and 16.1% at 800 °C. The principal source of 2-hydroxy-benzaldehyde was formed from dehydrogenation of guaiacol followed by C—O shift reaction and dehydrogenation reaction, which was promoted by higher temperature [25]. Yields of aromatic compounds such as benzene (5.5%), toluene (2.8%), and ethylbenzene (2.5%) were higher at 800 °C, for two possible reasons: the first was that the α-OH group was beneficial to the conversion of benzoic acid to benzene derivatives, since the yield of benzoic acid decreased from 9% to 0.6%; the second was that α-OH groups could be favorable for formation of small molecule olefins which can be converted to benzene derivatives through polymerization reactions at the higher temperature [26]. This can be verified by Fig. 4(b), which shows more olefins were generated from pyrolysis of α-OH-PPE-(*o*-OMe).

As to the pyrolysis of (*p*-methoxy + α-OH)-PPE-(*o*-OMe) at 500 °C, there were six major pyrolysis products: 2-hydroxy-benzaldehyde (20.2%), guaiacol (8.1%), 4-methoxy-styrene (31.3%), 4-methoxy-benzaldehyde (4.1%), 4-methoxy-acetophenone (19.6%), and 4-hydroxy-acetophenone (15.7%), which were mainly formed by breaking ether linkages and C—C bonds in the benzene ring. Compared to 500 °C, the number of products increased significantly at 800 °C, but the yield of 4-methoxy-styrene decreased a lot from 28.02% to 9.33%; also lower amounts of 4-methoxy-acetophenone, 4-hydroxy-acetophenone, and guaiacol were evident at the higher temperature. In contrast, the amounts of other compounds with simple substituents such as toluene, ethylbenzene, styrene, anisole, and benzaldehyde increased, particularly the yield of phenol, which increased to 17.1%.

The pyrolysis of phenethyl phenyl ether (PPE) takes place mainly through radical reactions, which can be divided into three types: Cβ-O homolytic reactions, Cα-Cβ homolytic reactions, and concerted reactions [27,28], all of which are shown in Fig. 6. The dissociation energy of Cβ-O was the lowest; therefore, the Cβ-O homolytic reaction dominated the entire reaction process in the pyrolysis. Fig. 6(a) shows that the intermediates, such as b1, b2, c1, and c2, were first generated by homolytic and hydrogen abstraction reactions, with the main products being styrene, phenol, benzaldehyde, and so on. However, during Cα-Cβ homolytic reactions (Fig. 6(b)), benzene, toluene, anisole, and other substances were obtained through a series of reactions after breaking the Cα—Cβ bond. In the concerted reaction (Fig. 6(c)), styrene and phenol were generated through path 1 by breaking the Cβ-O bond directly, and in the path 2, acetophenone was the main product through the cleavage of the $C_{4'}$—O bond and transfer of H from Cβ to $C_{4'}$.

Britt et al. [27] noted that the introduction of oxygen-containing substituents to both sides of the PPE benzene ring should not significantly alter the morphology and geometry of the precursors, transition states, and intermediates, but had a major impact on the pyrolysis rate and product selectivity [28,29]. Compared with α-OH-PPE-(*o*-OMe), the introduction of a methoxy group to the C_4 position could suppress the Cβ-O homolytic reaction (Fig. 6(a)) and promote the Cα-Cβ homolytic reaction (Fig. 6(b)) in (*p*-methoxy + α-OH)-PPE-(*o*-OMe) [30], leading to lower guaiacol content, but higher yields of 4-methoxy-benzaldehyde. Additionally, benzoic acid was generated at both 500 °C and 800 °C in α-OH-PPE-(*o*-OMe), while it was not detected in the other two samples. However, the pyrolysis of *p*-methoxy-PPE-(*o*-OMe) and

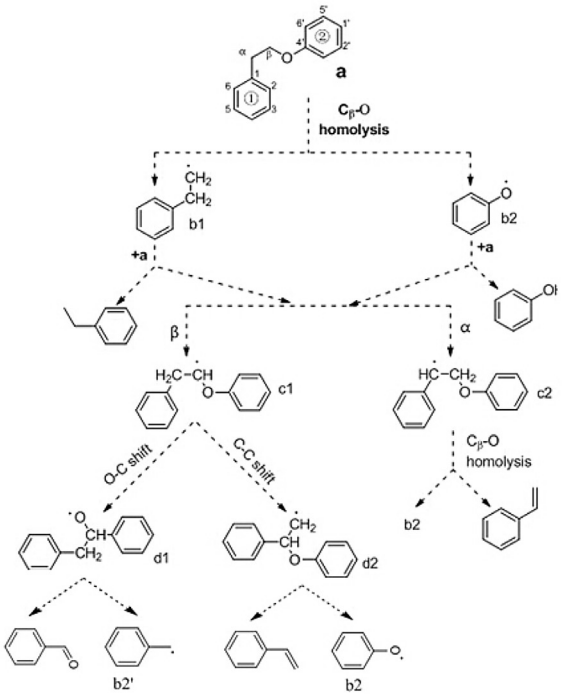

(a) C_β-O homolytic mechanism

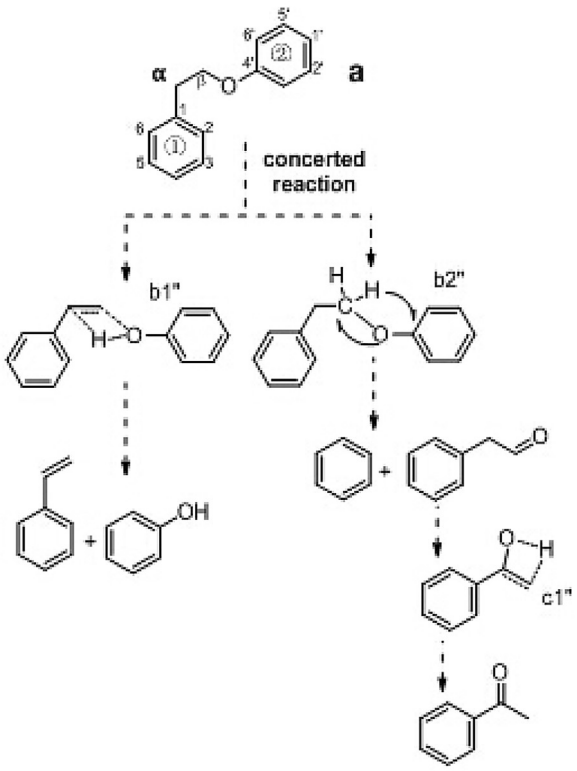

(c) Concerted reaction mechanism

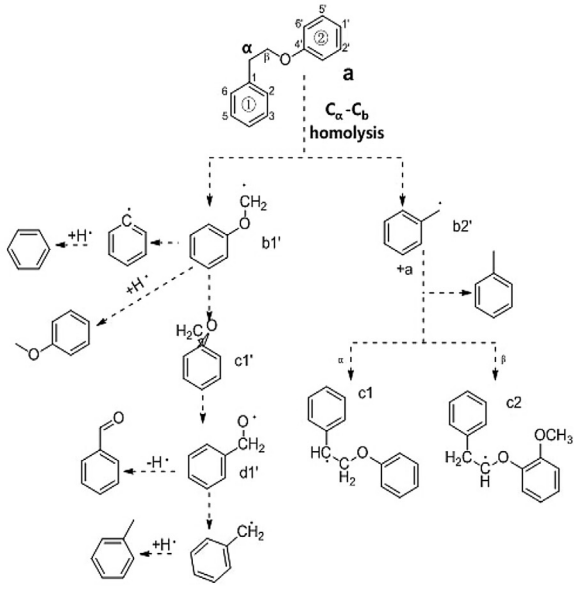

(b) C_α-C_β homolytic mechanism

Fig. 6. Radical reactions of PPE pyrolysis.

(*p*-methoxy + α-OH)-PPE-(*o*-OMe) at 500 °C showed that adding a hydroxyl group to the benzene ring could inhibit the generation of certain pyrolysis products such as toluene, ethylbenzene, anisole, benzaldehyde, and 4-ethyl-anisole to some extent, limiting the types of pyrolysis products and giving a more uniform distribution. At 500 °C, the 4-methoxy-styrene contents of *p*-methoxy-PPE-(*o*-OMe) and (*p*-methoxy + α-OH)-PPE-(*o*-OMe) were 36.1% and 31.3%, respectively, higher than the styrene content (26.3%) of α-OH-PPE-(*o*-OMe), while both the products were generated by a Cβ-O homolytic reaction followed by a C—C shift reaction [31]. Thus, it could be suggested that the presence of a methoxy group at the C_4 position could improve the selectivity of α/β [32,33]. Another possible pathway after Cβ-O homolytic reaction was a C—O shift reaction, with the main products being benzaldehyde and 2-hydroxy-benzaldehyde, which had combined yields of 15.2%, 18.4%, and 20.2% for *p*-methoxy-PPE-(*o*-OMe), α-OH-PPE-(*o*-

OMe)), and (*p*-methoxy + α-OH)-PPE-(*o*-OMe)) respectively, This was lower than the yields of the C—C shift reaction, which generated styrene derivatives, indicating that the energy barrier of the C—C shift reaction was lower than that of the C—O shift reaction. However, acetophenone and 4-methoxy-acetophenone were mainly obtained by concerted reaction of the β-O-type models (see Fig. 6(c)), the content of acetophenone was only 0.3% in *p*-methoxy-PPE-(*o*-OMe), but the yields of acetophenone and 4-methoxy-acetophenone were 16.7% and 19.6% in α-OH-PPE-(*o*-OMe) and (*p*-methoxy + α-OH)-PPE-(*o*-OMe), respectively, which corresponded well with the results of the in-situ diffuse reflectance infrared pyrolysis. This indicates that α-OH was beneficial for the promotion of the generation of aromatic ketones from β-O-type models [34–36].

4. Conclusion

The influence of substituents on the pyrolysis of β-O-4 type model compounds and derivatives was investigated with pyroprobe-GC–MS and an in-situ diffuse reflectance infrared pyrolysis device. The main conclusions can be summarized as follows:

(1) Cβ-O homolytic reactions dominate the pyrolysis of phenethyl phenyl ether (PPE), consisting mainly of C—C shift and C—O shift reactions.
(2) In β-O-4 model compound pyrolysis, the introduction of α-OH promoted the generation of aryl-ketone products; the methoxy group on the aromatic ring represented an unstable site and restructuring and homolytic reactions occurred there at temperatures over 500 °C. The co-existence of α-OH and *p*-methoxy groups had a role in the inhibition of decarbonylation.
(3) The introduction of oxygen-containing substituents to both sides of the PPE benzene ring resulted in a major impact on both the rate of pyrolysis and product selectivity. The presence of a methoxy group at the C_4 position contributed to the generation of styrene/4-methoxy styrene by homolytic and hydrogen abstraction reactions. α-OH was beneficial for promotion of concerted reactions and the generation of acetophenone/4-methoxy-acetophenone by breaking $C_{4'}$—O bond and transferring H from Cβ to $C_{4'}$ in β-O-4 type models.

Acknowledgements

This research project was financially supported by the National Basic Research Program of China (2013CB228102), the National Natural Science Foundation of China (NO. 51376075 and 51506071), the Foundation of State Key Laboratory of Coal Combustion (FSKLCCB1504) and the Fundamental Research Funds for the Central Universities. Assistance from the Analysis and Testing Center of HUST is highly appreciated.

References

[1] A.J. Ragauskas, G.T. Beckham, M.J. Biddy, R. Chandra, F. Chen, M.F. Davis, B.H. Davison, R.A. Dixon, P. Gilna, M. Keller, Science 344 (2014) 1246843.
[2] J. Yanik, R. Stahl, N. Troeger, A. Sinag, J. Anal. Appl. Pyrolysis 103 (2013) 134.
[3] A.V. Bridgwater, Biomass Bioenergy 38 (2012) 68.
[4] A. Bridgwater, H. Gerhauser, A. Effendi, in, Google Patents, 2011.
[5] H. Yang, R. Yan, H. Chen, D.H. Lee, C. Zheng, Fuel 86 (2007) 1781.
[6] S. Mukkamala, M.C. Wheeler, A.R. van Heiningen, W.J. DeSisto, Energy Fuels 26 (2012) 1380.
[7] J. Huang, C. He, J. Anal. Appl. Pyrolysis 113 (2015) 655.
[8] T. Nakamura, H. Kawamoto, S. Saka, J. Anal. Appl. Pyrolysis 81 (2008) 173.
[9] J. Reiter, H. Strittmatter, L.O. Wiemann, D. Schieder, V. Sieber, Green Chem. 15 (2013) 1373.
[10] S. Chu, A.V. Subrahmanyam, G.W. Huber, Green Chem. 15 (2013) 125.
[11] P.F. Britt, A. Buchanan, M.J. Cooney, D.R. Martineau, J. Org. Chem. 65 (2000) 1376.
[12] J. Huang, C. Liu, D. Wu, H. Tong, L. Ren, J. Anal. Appl. Pyrolysis 109 (2014) 98.
[13] H. Kawamoto, M. Ryoritani, S. Saka, J. Anal. Appl. Pyrolysis 81 (2008) 88.
[14] A. Beste, A. Buchanan Iii, R.J. Harrison, J. Phys. Chem. A 112 (2008) 4982.
[15] A.G. Sergeev, J.F. Hartwig, Science 332 (2011) 439.
[16] J. Buendia, J. Mottweiler, C. Bolm, Chem. A Eur. J. 17 (2011) 13877.
[17] S. Wang, K. Wang, Q. Liu, Y. Gu, Z. Luo, K. Cen, T. Fransson, Biotechnol. Adv. 27 (2009) 562.
[18] L. Chen, X. Wang, H. Yang, Q. Lu, D. Li, Q. Yang, H. Chen, J. Anal. Appl. Pyrolysis 113 (2015) 499.
[19] T. Hosoya, H. Kawamoto, S. Saka, J. Anal. Appl. Pyrolysis 84 (2009) 79.
[20] T. Hosoya, H. Kawamoto, S. Saka, J. Anal. Appl. Pyrolysis 83 (2008) 78.
[21] Z. Luo, S. Wang, X. Guo, J. Anal. Appl. Pyrolysis 95 (2012) 112.
[22] G. Lv, S. Wu, G. Yang, J. Chen, Y. Liu, F. Kong, J. Anal. Appl. Pyrolysis 104 (2013) 185.
[23] L. Chen, X. Ye, F. Luo, J. Shao, Q. Lu, Y. Fang, X. Wang, H. Chen, J. Anal. Appl. Pyrolysis 115 (2015) 103.
[24] S. Zhou, M. Garcia-Perez, B. Pecha, A.G. McDonald, S.R. Kersten, R.J. Westerhof, Energy Fuels 27 (2013) 1428.
[25] S. Zhou, M. Garcia-Perez, B. Pecha, S.R. Kersten, A.G. McDonald, R.J. Westerhof, Energy Fuels 27 (2013) 5867.
[26] C. Mukarakate, J.D. McBrayer, T.J. Evans, S. Budhi, D.J. Robichaud, K. Iisa, J. ten Dam, M.J. Watson, R.M. Baldwin, M.R. Nimlos, Green Chem. 17 (2015) 4217.
[27] P.F. Britt, M.K. Kidder, A. Buchanan Iii, Energy Fuels 21 (2007) 3102.
[28] J.M. Younker, A. Beste, A. Buchanan, ChemPhysChem 12 (2011) 3556.
[29] J. Asomaning, P. Mussone, D.C. Bressler, J. Anal. Appl. Pyrolysis 105 (2014) 1.
[30] A. Beste, A. Buchanan III, J. Organic Chem. 74 (2009) 2837.
[31] B. Holmelid, M. Kleinert, T. Barth, J. Anal. Appl. Pyrolysis 98 (2012) 37.
[32] R. Hubaut, M. Daage, J. Bonnelle, Appl. Catal. 22 (1986) 231.
[33] H. Wu, S. Radomkit, J.M. O'Brien, A.H. Hoveyda, J. Am. Chem. Soc. 134 (2012) 8277.
[34] V.Y. Korobkov, E.N. Grigorieva, V.I. Bykov, O.V. Senko, I.V. Kalechitz, Fuel 67 (1988) 657.
[35] A.T. To, R.E. Jentoft, W.E. Alvarez, S.P. Crossley, D.E. Resasco, J. Catal. 317 (2014) 11.
[36] B.M. Laloo, H. Mecadon, M.R. Rohman, I. Kharbangar, I. Kharkongor, M. Rajbangshi, R. Nongkhlaw, B. Myrboh, J. Org. Chem. 77 (2011) 707.